PFC/JA-91-3

Steady State and Time Dependent Effects of Fusion Reactivity Enhancement due to Minority Heating in D-T and D-^{3}He Tokamak Plasmas

E. A. Chaniotakis
D. J. Sigmar

February 1991

Plasma Fusion Center
Massachusetts Institute of Technology
Cambridge, Massachusetts 02139 USA

This work was supported by DOE grant DE-FG02-91ER-54109.

Steady State and Time Dependent Effects of Fusion Reactivity Enhancement due to Minority Heating in D-T and D-^{3}He Tokamak Plasmas

E.A. Chaniotakis, D.J. Sigmar
MIT Plasma Fusion Center

ABSTRACT

In D-T and D-^{3}He plasmas ICRF heating at the second harmonic of deuterium results in the modification of the distribution function of the heated ions. This report describes the effects of this distribution function modification on the steady state and dynamic behavior of plasmas. The theory of tail formation due to ICRF heating is summarized and its effect on the fusion reaction rate is presented. Using a 0-D plasma transport model the effect of ICRF heating on the plasma operating contours is analyzed for the CIT, ITER, and a D-^{3}He tokamak. In analyzing the dynamic behavior, a model for the characteristic time of tail relaxation, τ_ξ, is developed and a feedback model based on auxiliary power is presented. The stabilization of temperature perturbations in a D-^{3}He plasma is simulated under various values of τ_ξ.

1 Introduction

As the world fusion program is approaching the burning plasma state there is increasing interest in understanding plasma operating point control and thermal instability. Strong auxiliary heating power P_{aux} is required to cross the Cordey pass and – if ICRH is used – the ensuing energetic minority ion tail will affect the fusion reactivity and hence the burn dynamics, particularly if the main burn control system relies on tailoring P_{aux} dynamically in response to thermal excursions.

Dawson, Furth and Tunney [1] were the first to point out the fusion reactivity enhancement due to auxiliary (N.B.I.) heating. Latter, following the ground breaking work of Stix [2] who theoretically demonstrated

ion tail formation due to ICRH, Kesner [3] performed an investigation of the combined effect of NBI and ICRH driven fuel ion distribution function distortions on the thermonuclear energy multiplication factor Q. More recently, Blackfield and Scharer [4] applied a 2-D (in velocity space), 0-D (in configuration space) Fokker-Planck ICRF code to (PLT and) the hypothetical NUWMAK tokamak reactor and found little Q enhancement due to deuteron minority heating for their parameter regime. Later, Scharer et. al. [5] performed a specific analysis for JET with fundamental deuteron minority heating in a tritium plasma resulting in a $1.6 - 1.9$ fusion power enhancement after a 1 sec heating pulse.

Using their bounce averaged Fokker-Planck quasilinear code, Harvey et. al. [6] analyzed second harmonic heating of a 50:50 D-T plasma. Depending on the chosen density, the ion tail can be pushed out beyond the maximum of the D-T $\langle \sigma_f v \rangle$ curve. At values of $Q < 1$ sizable ion tail driven enhancement factors of the reactivity can be obtained but at $Q > 1$ the enhancement decreases rapidly, in this ICRH heating scenario.

Returning to minority heated fusion plasma scenarios, we focus in the present work on a different novel aspect, i.e. the problem of operating point control in tokamaks relying on variable ICRH heating for burn control. Besides burn control it appears that the resulting phase lag of the plasma temperature time response can yield important information on energy equilibration and confinement time of the main ions, the minority and the fusion products.

In Section 2 we develop the problem by starting with the Stix formula for the energetic ion tail driven by ICRH. In Section 3 we pursue its consequences for the fusion reactivity $\langle \sigma_f v \rangle$ averaged over a fuel ion distribution function with effective temperature $T_{eff} = T/\mathcal{F}(\xi)$ where $\xi \propto P_{icrh}\sqrt{T_e}/n_e^2$ is the Stix parameter and $\mathcal{F}$ is a known function. In Section 4 we implement the ICRH enhanced fusion power source term in the 0-D plasma power balance in a space spanned by plasma density and temperature and analyze the self-consistent (nonlinear in P_{icrh}) steady state solutions of the plasma

power balance for three tokamaks resembling (a) CIT, (b) ITER and (c) a 10 Tesla, $R_0 = 6.3$ m D-^{3}He advanced reactor design, see Table 1. In Section 5, the 0-D steady state power balance of Section 4 is extended to the time dependent case to study the dynamic effects of the energetic ion tail equilibration with the bulk plasma and its implications for operating point control using a simple feedback law but including the delayed additional heating power input from the ICRH minority tail. Sections 6 contains a summary and conclusions.

2 Distribution function modifications due to ICRH

Before the distribution function, derived Appendix A, is used to calculate the fusion reactivity and the plasma performance it is useful to investigate the effect of the various plasma parameters on the shape of the distribution function. From Eq. 47 it is apparent that the parameter ξ depends on the applied ICRF power density, (P_{ICRF}), and on the plasma density and temperature, i.e.

$$\xi = \xi\left(\langle P_{\mathrm{ICRF}}\rangle, T, n\right) \tag{1}$$

and in particular ξ follows the scaling

$$\xi \sim \frac{\langle P_{\mathrm{ICRF}}\rangle T_e^{1/2}}{n_e^2}, \tag{2}$$

As ξ increases the distribution function deviates increasingly from the Maxwellian. The deviation becomes pronounced for $\xi \geq 1$, and thus it is important to determine the values of the density, temperature and ICRF heating power density that result in $\xi = 1$. The relation between ξ, n, T, and $\langle P_{\mathrm{ICRF}}\rangle$ is shown in Fig. 1 where the $\xi = 1$ contour is shown in the density-temperature operating space for a D-T plasma for various values of $\langle P_{\mathrm{ICRF}}\rangle$.

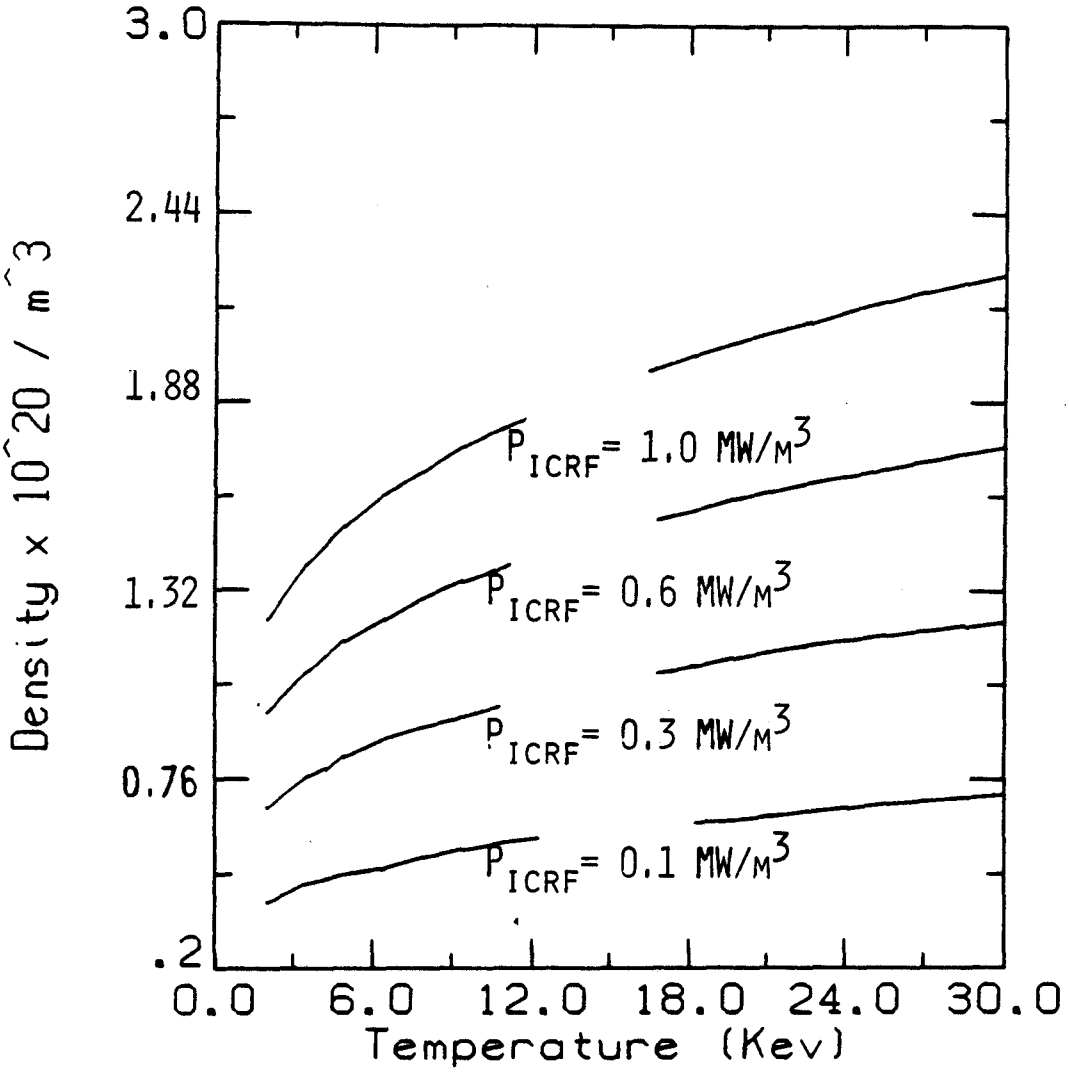

Figure 1: The contours $\xi = 1$ for the various values of ICRF heating power density indicated on each contour.

Two contours on Fig. 1 are of significant importance. The contour labeled 0.1 MW/m^3 corresponds approximately to the power density for the technology phase of the ITER tokamak, and the contour labeled 0.6 MW/m^3 corresponds to the power density of the CIT tokamak. Note that as the power density increases the $\xi = 1$ contour encompasses more of the density - temperature operating space.

As an example of the change in the distribution function of ions heated by ICRF, a D-^{3}He plasma is considered with the following parameters.

$$\begin{aligned}
&\text{Electron density} && n_e = 0.7 \times 10^{20}/m^3 \\
&\text{Deuterium density} && n_D = \frac{1}{3} 0.7 \times 10^{20}/m^3 \\
&\text{Tritium density} && n_T = \frac{1}{3} 0.7 \times 10^{20}/m^3 \\
&\text{Electron temperature} && T_e = 50\text{keV} \\
&\text{Heating power} && \langle P_{\text{ICRF}} \rangle = 0.11\text{MW/m}^3
\end{aligned} \tag{3}$$

The value of the parameter ξ is a function of the electron temperature and the dependance is shown in Fig. 2. Note that ξ increases with temperature as indicated by Eq. 47. For reference, a plot of the function H, given by Eq. 50, is shown on Fig. 3.

For the plasma parameters indicated above the distribution function of the heated deuterium ions is shown on Fig. 4. The dotted line represents the distribution due to ICRF heating and the solid line corresponds to a Maxwellian distribution. Note that the change in the distribution function due to ICRF, for the D-^{3}He plasma under investigation, is significant for this case.

3 Effect of ICRF heating on the fusion reaction rate

In the previous section the change in the distribution function of ICRF heated ions was shown to be significant under certain circumstances when

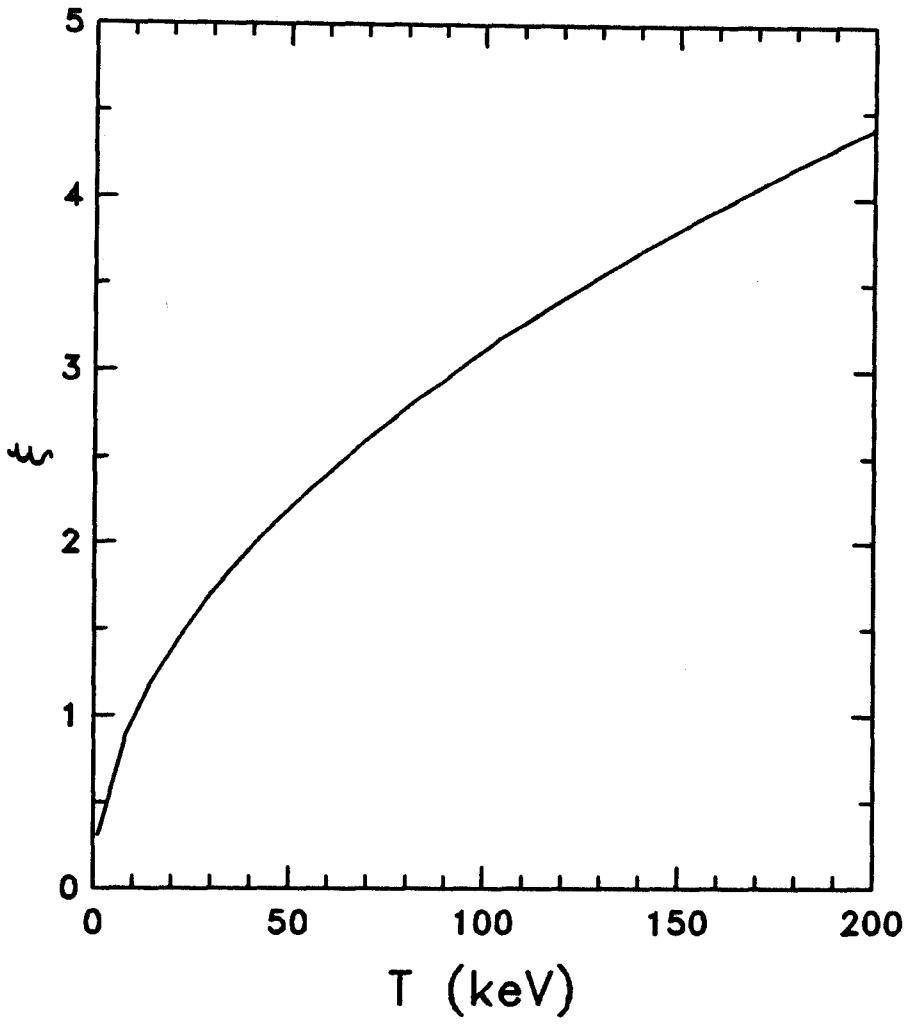

Figure 2: A plot of the parameter ξ as a function of plasma background temperature for a D-^{3}He plasma heated by .11 MW/m^3 of ICRF power. The density of the deuterium and tritium ions is 0.23×10^{20}/m^3.

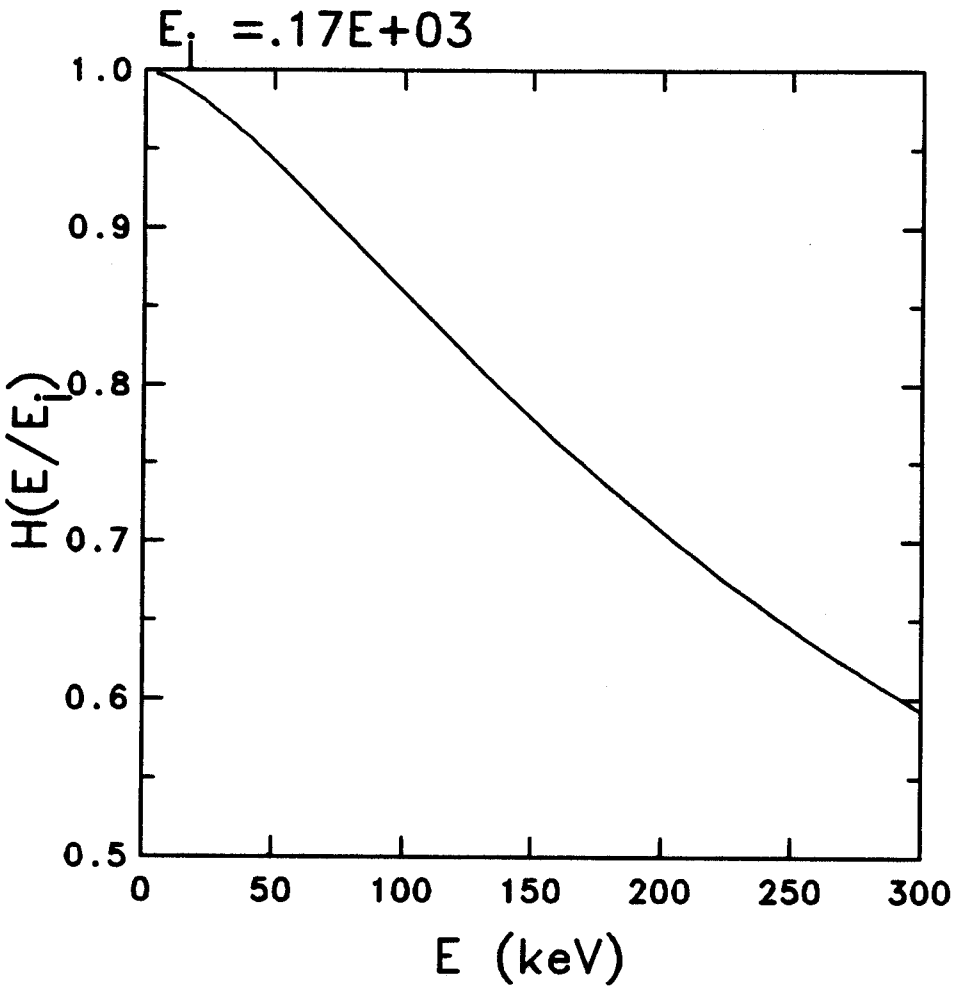

Figure 3: A plot of the function H (see Eq. 50) for a D - ^{3}He plasma as a function of the energy of the resonant ions. The corresponding value of ξ is 2.2.

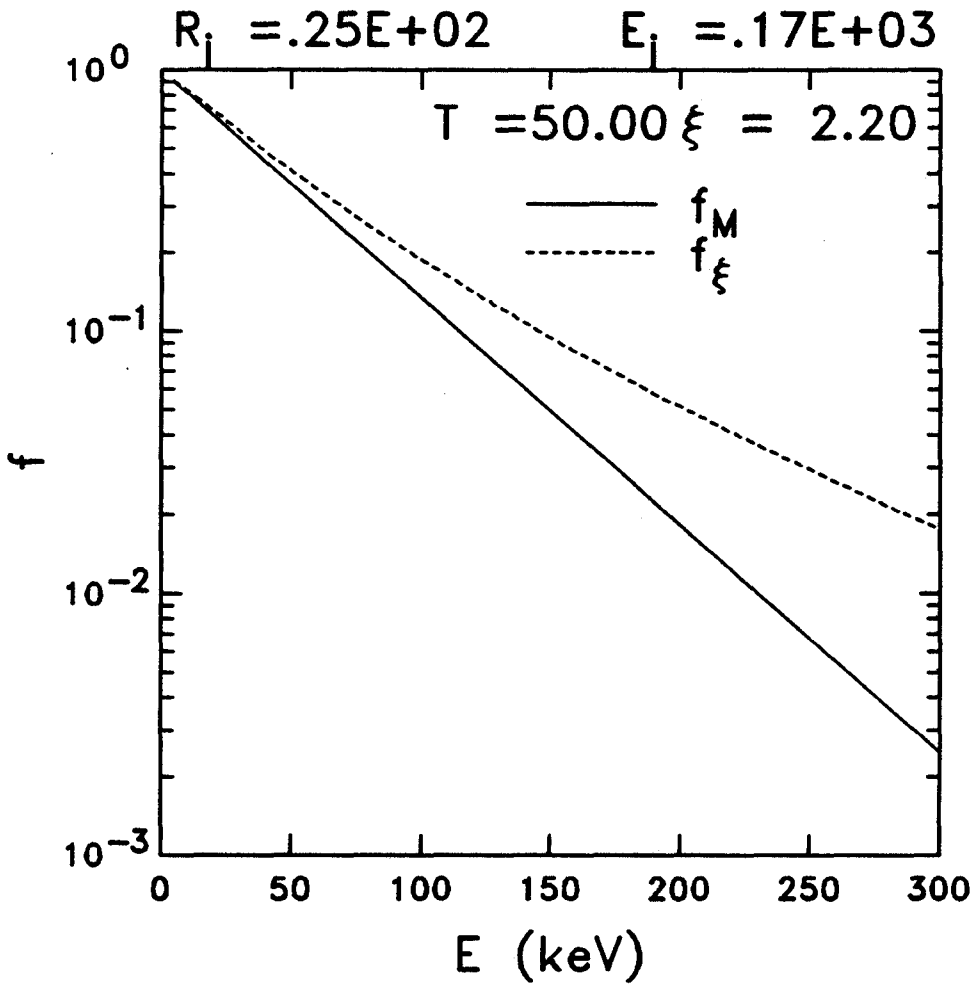

Figure 4: Normalized distribution function of Maxwellian (solid line) and ICRF heated deuterium ions in a D-^{3}He plasma with an assumed background temperature of 50 keV. The ICRF power density is .11 MW/m^3 and the density of the deuterium and tritium ions is 0.23×10^{20}/m^3. Expressions for the parameters R_j and E_j are given by Eqs. 48 and 49 respectively.

compared with the equivalent Maxwellian distribution function. This change in the distribution function results in changes in the fusion reactivity $\langle \sigma v \rangle$ which in turn affects the fusion reaction rate and thus the overall plasma power balance.

The reaction rate, R, of a thermonuclear plasma depends on the reactivity of the interacting particles and on their density. In particular if the plasma is composed of particles of two species with density n_1 and n_2 the reaction rate is given by

$$R_{12} = n_1 n_2 \langle \sigma v \rangle \tag{4}$$

The reactivity $\langle \sigma v \rangle$ is given by

$$\langle \sigma v \rangle = 4\pi \left(\frac{m_r}{2\pi T} \right)^{3/2} \int_0^\infty \exp \left[\left(-\frac{m_r v^2}{2T} \right) \mathcal{F}(\xi) \right] v^3 \sigma(v)\, dv \tag{5}$$

In the above equation $m_r = m_1 m_2/(m_1 + m_2)$ is the reduced mass of the reacting particles and T is the temperature of the background ions. For a plasma whose species are characterized by Maxwellian distributions the function $\mathcal{F}(\xi)$ is equal to unity. However, for ICRF heated plasmas the function $\mathcal{F} < 1$ and thus the resulting reactivity differs from the reactivity of pure Maxwellian plasmas. Equation 5 can be written in terms of the particle energy E in the center of mass reference frame as follows

$$\langle \sigma v \rangle = \frac{4}{\sqrt{2\pi m_1}} \left(\frac{m_r}{m_1 T} \right)^{3/2} \int_0^\infty \exp \left[\left(-\frac{m_r E}{m_1 T} \right) \mathcal{F}(\xi) \right] E\, \sigma(E)\, dE \tag{6}$$

Once the cross section σ of the reaction is characterized, Eq. 6 determines the reactivity. In this analysis we evaluate the reactivity of D-T and D-^{3}He plasmas with expressions for their cross sections given in Appendix B.

For Maxwellian plasmas the reactivity $\langle \sigma v \rangle$ is independent of the plasma density, but for ICRF heated plasmas the function $\mathcal{F}$, and thus the reactivity, depend on the plasma density cf.Eq. 44. The following examples are considered:

D-T Plasma	D-^{3}He Plasma
$n_e = 0.7 \times 10^{20}/m^3$	$n_e = 0.7 \times 10^{20}/m^3$
$n_D = \frac{0.7}{2} \times 10^{20}/m^3$	$n_D = \frac{0.7}{3} \times 10^{20}/m^3$
$n_T = \frac{0.7}{2} \times 10^{20}/m^3$	$n_{^3\mathrm{He}} = \frac{0.7}{3} \times 10^{20}/m^3$
$\langle P_{\mathrm{ICRF}} \rangle = 0.11\,\mathrm{MW/m^3}$	$\langle P_{\mathrm{ICRF}} \rangle = 0.11\,\mathrm{MW/m^3}$

(7)

In Fig. 5 the reactivity of the D-T plasma, whose parameters are given in (7), is shown for the cases when both the deuterium and tritium ions are characterized by a Maxwellian distribution, and when the deuterium ions are heated by 0.11 MW/m^3 of ICRF waves. A similar plot for the reactivity of a D-^{3}He plasma is shown on Fig. 6.

4 Steady state issues: Operating point selection including ICRF produced ion tail

In the analysis that follows the performance of tokamak plasmas is investigated with the aide of a volume averaged (0-D) plasma transport model. In such a model, the plasma density and temperature are characterized by fixed profile shapes and the averaging is performed over the plasma volume. In general the 0-D power balance of the ohmic P_Ω, the fusion P_f, the auxiliary $P_u x a$, the conduction losses P_l, the Bremsstrahlung radiation P_B and the synchrontron radiation P_s power densities, of a plasma of elliptic cross section with elongation κ and with parabolic density and temperature profiles that is characterized by the exponents ν_n and ν_T respectively, are given by

$$\frac{0.024}{1+\nu_n+\nu_T}(n_{e,0}+n_{i,0})\frac{\partial T_0}{\partial t} = P_\Omega + \eta_f P_f + P_{aux} - P_l - P_B - P_s \qquad (8)$$

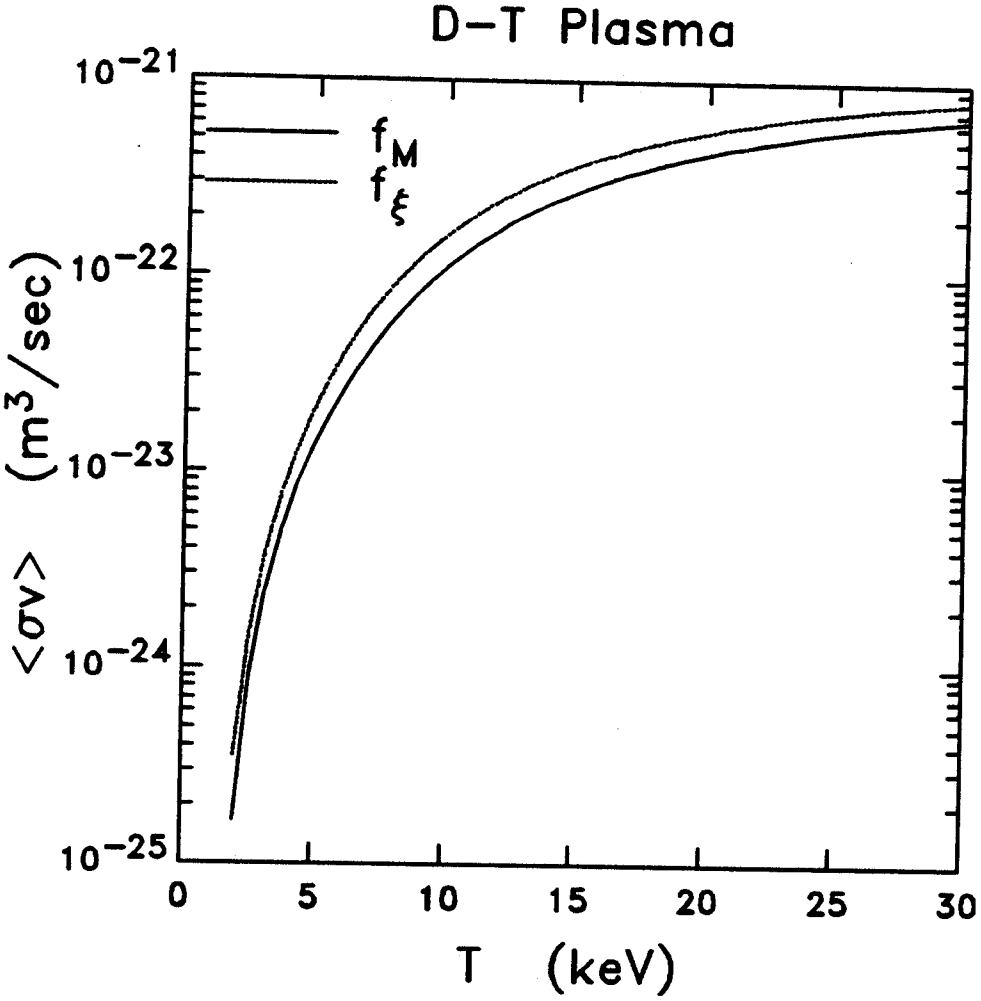

Figure 5: The reaction rate $\langle \sigma v \rangle$ as a function of plasma temperature for a D-T plasma characterized by Maxwellian distribution functions (solid curve) and for a D-T plasma whose deuterium ions are heated by 0.11 MW/m^3 of ICRF power.

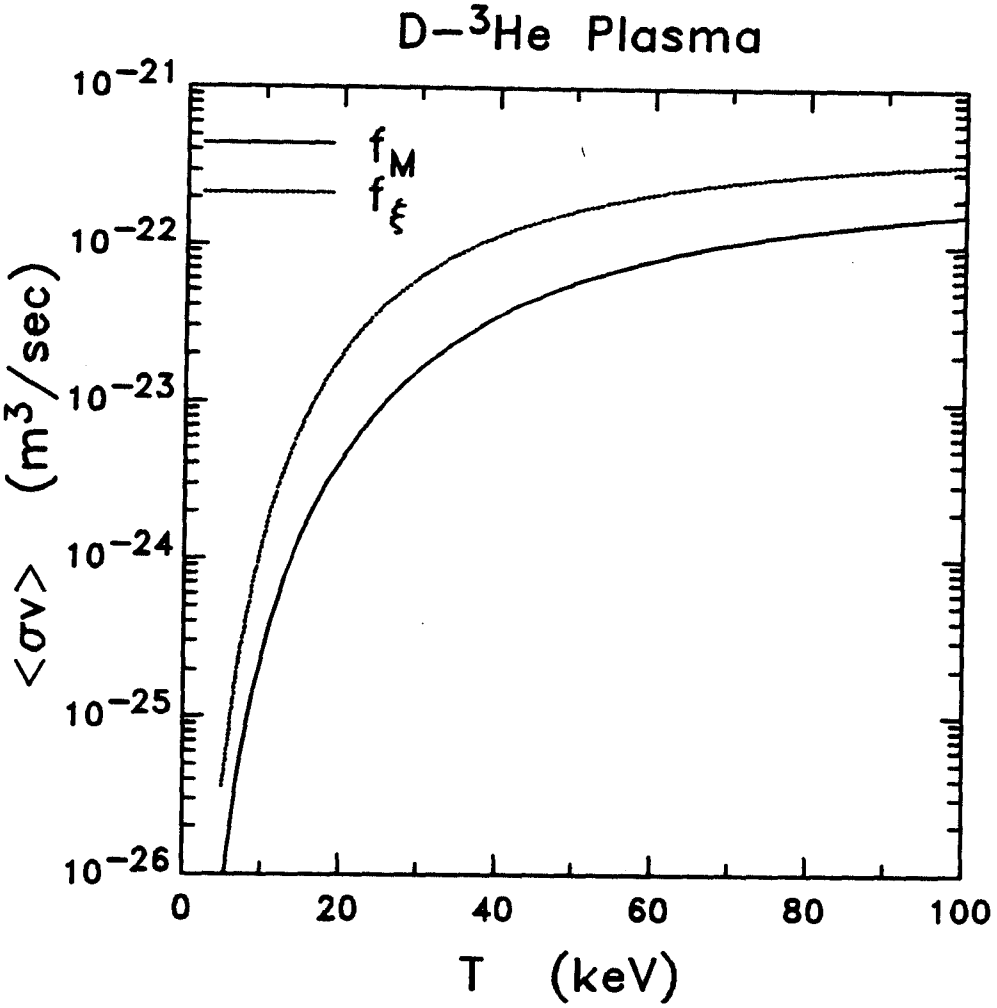

Figure 6: The reaction rate $\langle \sigma v \rangle$ as a function of plasma temperature for a D-^{3}He plasma characterized by Maxwellian distribution functions (solid curve) and for a D-^{3}He plasma whose deuterium ions are heated by 0.11 MW/m^3 of ICRF power.

With the temperature given in units of keV and the density in units of $10^{20}/m^3$ the terms on the right hand side of Eq. 8 become

$$P_\Omega = 0.01045 \frac{\ln\Lambda\, Z_{eff}}{1+1.5\nu_T}\left(\frac{1+\kappa^2}{\kappa}\right)^2 \frac{B_0^2}{R_0^2 T_{e_0}^{3/2}} \tag{9}$$

$$P_l = \frac{0.024}{1+\nu_n+\nu_T}\frac{(n_{e_0}+n_{i_0})T_{e_0}}{\tau_E} \tag{10}$$

$$P_B = \frac{.0053 Z_{eff}}{2\nu_n+0.5\nu_T+1} n_{e_0}^2 T_{e_0}^{1/2} \tag{11}$$

$$P_s \simeq 0.00621 \frac{n_{e_0}T_{e_0}}{1+\nu_n+\nu_T} B_0^2 \left(1+\frac{T_{e_0}}{146(1+\nu_n+\nu_T)}\right) \tag{12}$$

where $\ln\Lambda$, Z_{eff}, B_0, and R_0 are respectively the Coulomb logarithm, the effective charge, the magnetic field on axis, and the plasma major radius.

For a D-T plasma P_f corresponds to the alpha power P_α which is given by

$$P_f \equiv P_\alpha = \frac{0.56}{\nu_T} n_{d,0} n_{t,0} F_f(T_0) \tag{13}$$

For a D-^{3}He plasma the fusion power is given by

$$P_f = \frac{2.928}{\nu_T} n_{d,0} n_{^3He,0} F_f(T_0) \tag{14}$$

The function $F_f(T_0)$ is given by

$$F_f(T_0) = \frac{10^{22}}{T_0^{(2\nu_n+1)/\nu_T}} \int_0^{T_0} \overline{\sigma v}(T) T^{(2\nu_n+1)/\nu_T - 1}\, dT \tag{15}$$

The plasma self heating efficiency η_f allows for less than perfect coupling of the charged fusion product power P_f to the bulk plasma. In the present work it is assumed that $\eta_f = 1$ throughout.

The energy confinement time τ_E is a combination between the ohmic (Neo-Alcator) [7] scaling τ_{NA} and the auxiliary scaling τ_{AU}. In this analysis the inverse quadrature form is used in order to limit the energy confinement time to the ohmic value.

$$\frac{1}{\tau_E} = \left(\frac{1}{\tau_{NA}^2} + \frac{1}{\tau_{AU}^2} \right)^{1/2} \tag{16}$$

The Neo-Alcator confinement scaling is given by

$$\tau_{NA} = 0.2 \overline{n}_e a R_0^2 \kappa^{.5} \tag{17}$$

In this analysis the auxiliary scaling is given by the ITER89P [8] energy confinement scaling

$$\tau_{AU} = 0.048\, H\, \frac{I_P^{0.85} R_0^{1.2} a^{0.3} \kappa^{0.5} \overline{n}_e^{0.1} B_0^{0.2} A_i^{0.5}}{(P_{aux} + P_f)^{0.5}} \tag{18}$$

Here H represents the H-mode enhancement factor, I_P is the total plasma current in MA, a is the plasma minor radius, A_i is the average atomic mass number of the plasma ions, and P_{aux} is the auxiliary power in MW.For a D-T plasma P_f is the alpha power in MW and for a D-^{3}He plasma P_f is the total fusion power in MW.

By setting $\partial T_0/\partial t = 0$ in Eq. 8 the effect of ICRF heating on plasma performance is investigated in the density-temperature operating space of the tokamaks whose parameters are given in Table 1.

By solving Eq. 8 for the auxiliary power in the density - temperature operating space we can obtain both the plasma operating contours (POPCON) and the contours of constant ξ for the parameters given in Table 1. These contours are shown on Figs. 7, 8, 9, 10, 11, 12 for the CIT, ITER, and D-^{3}He tokamaks.

Large values of ξ imply significant alteration of the resonant ions distribution function (see Eq. 44) which in turn results in appreciable changes

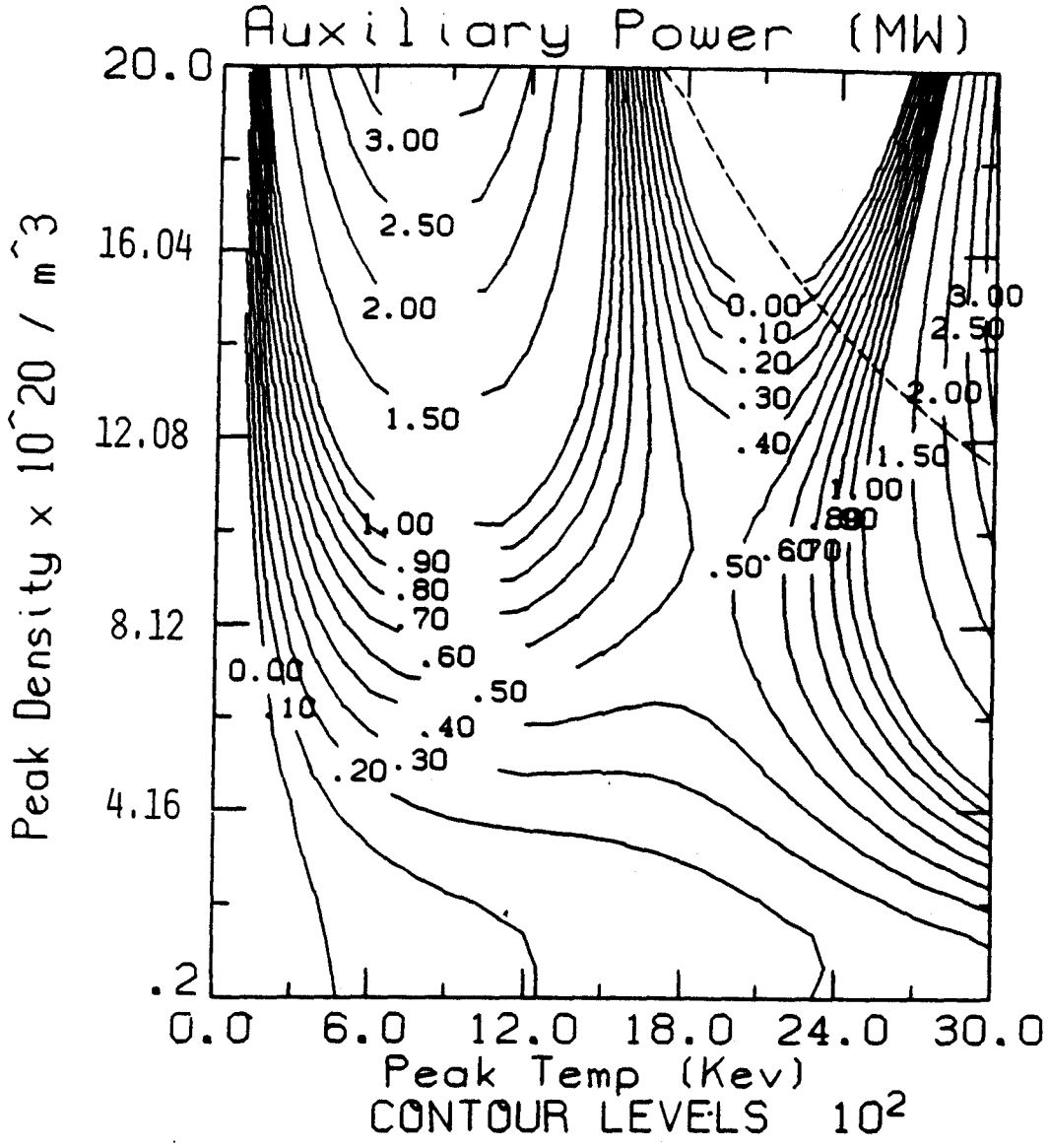

Figure 7: CIT density-temperature operating space with contours of auxiliary power. The dashed line corresponds to the β limit $3\,I_p/aB_0$

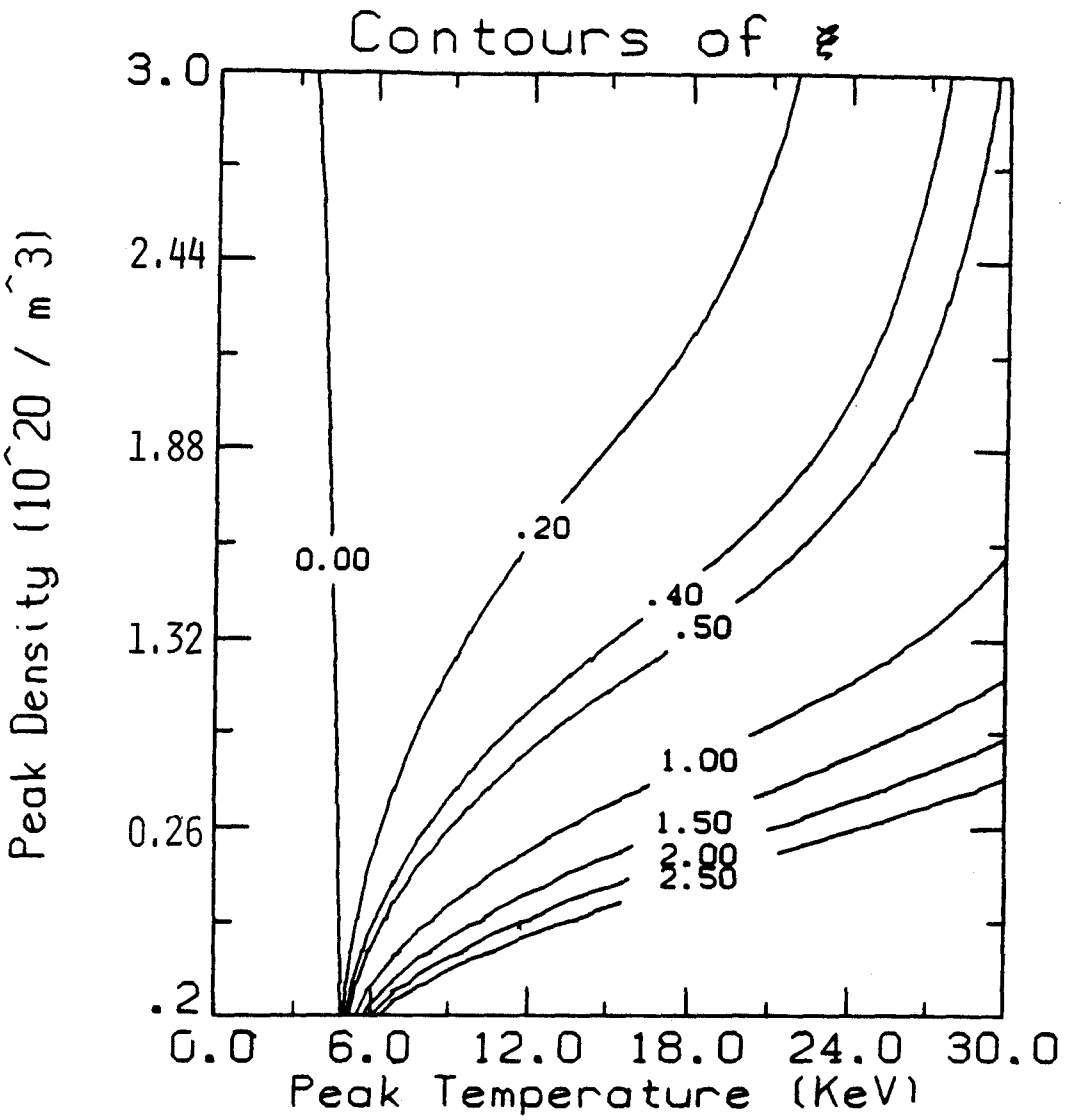

Figure 8: CIT contours of constant ξ (cf. Eq. 47) for D-T fusion. The P_{ICRF} values needed in evaluating ξ are taken from Fig. 7 at each value of density and temperature.

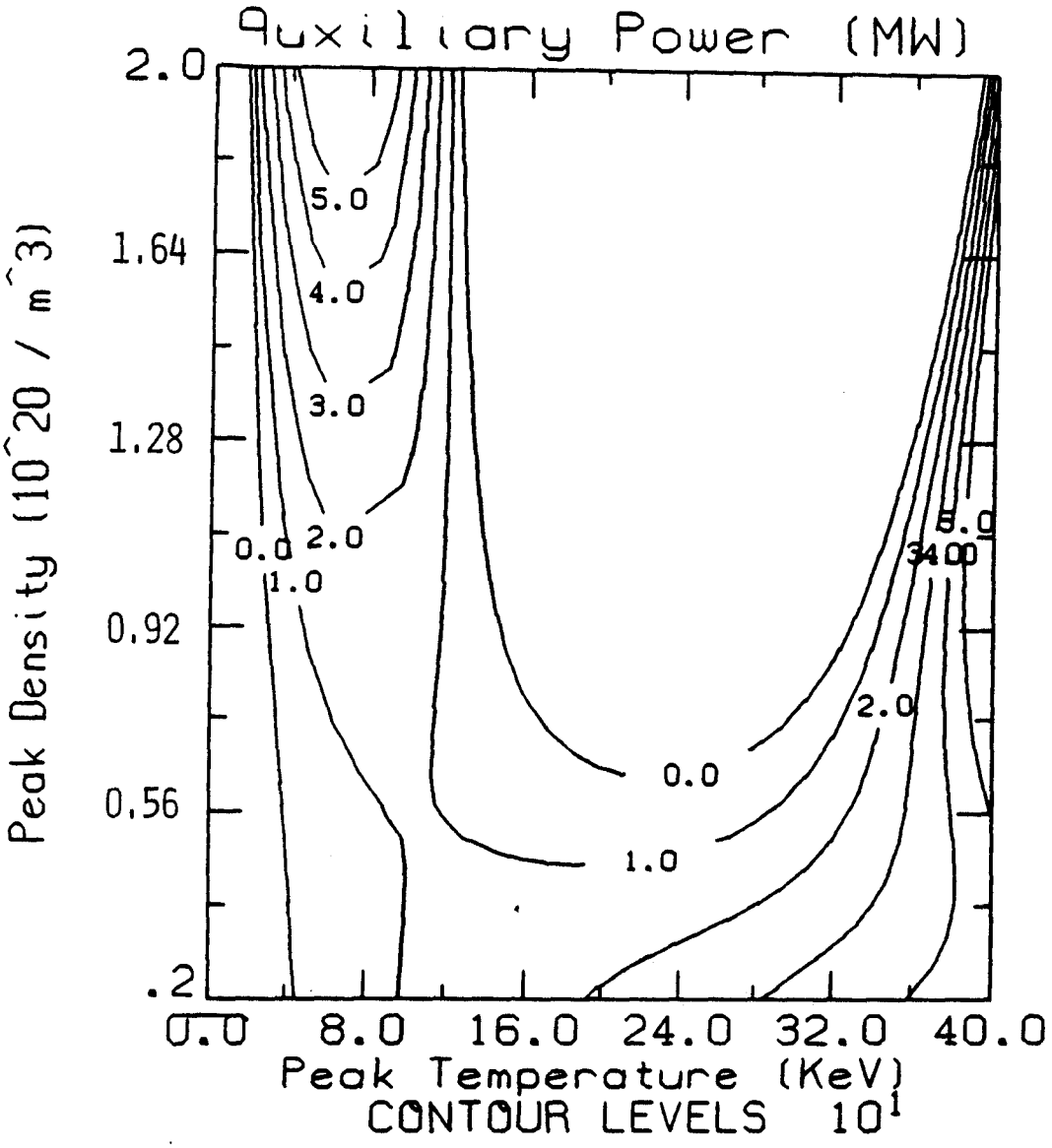

Figure 9: ITER density-temperature operating space with contours of auxiliary power.

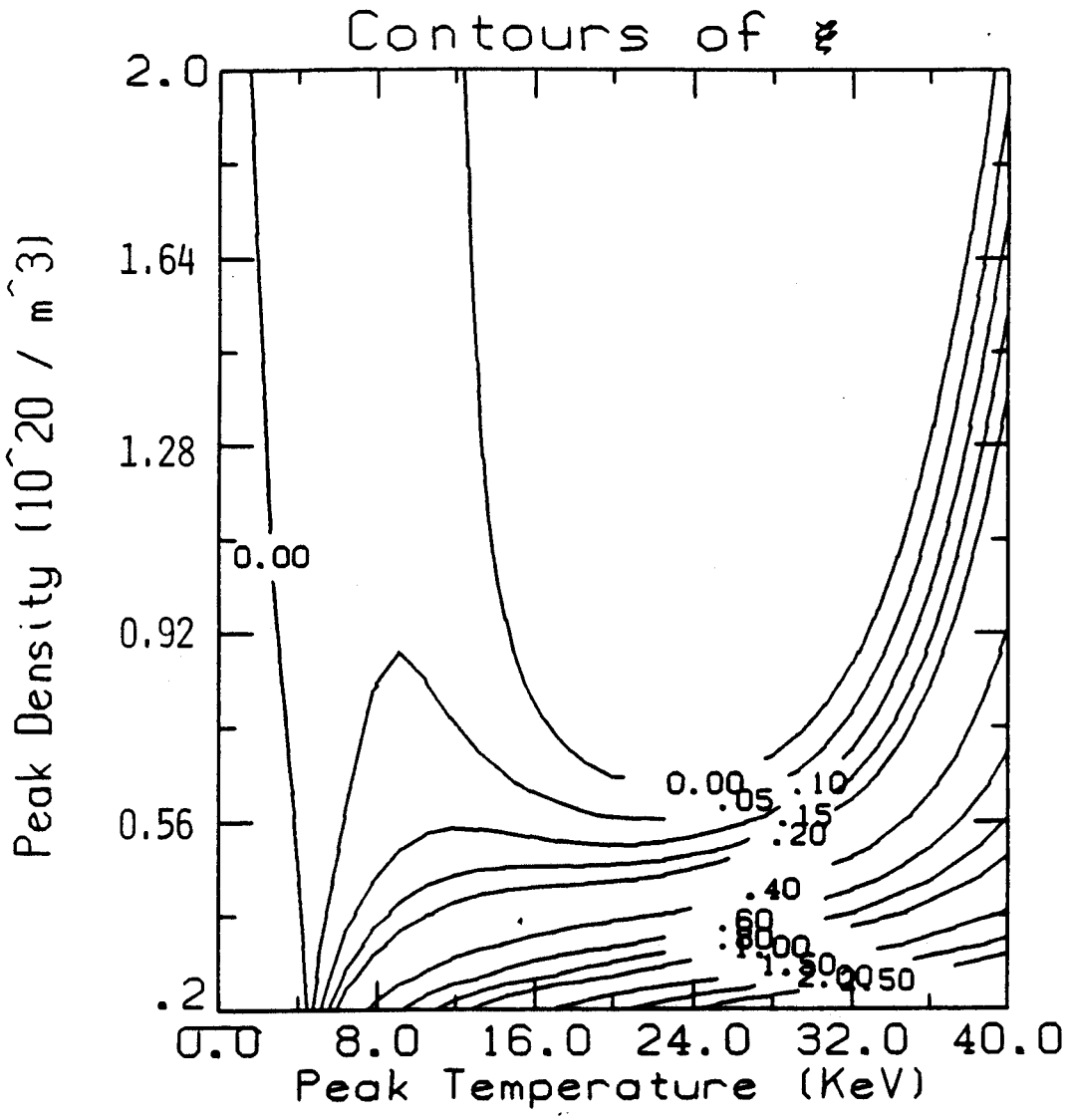

Figure 10: ITER contours of constant ξ (cf. Eq. 47) for D-T fusion. The P_{ICRF} values needed in evaluating ξ are taken from Fig. 7 at each value of density and temperature.

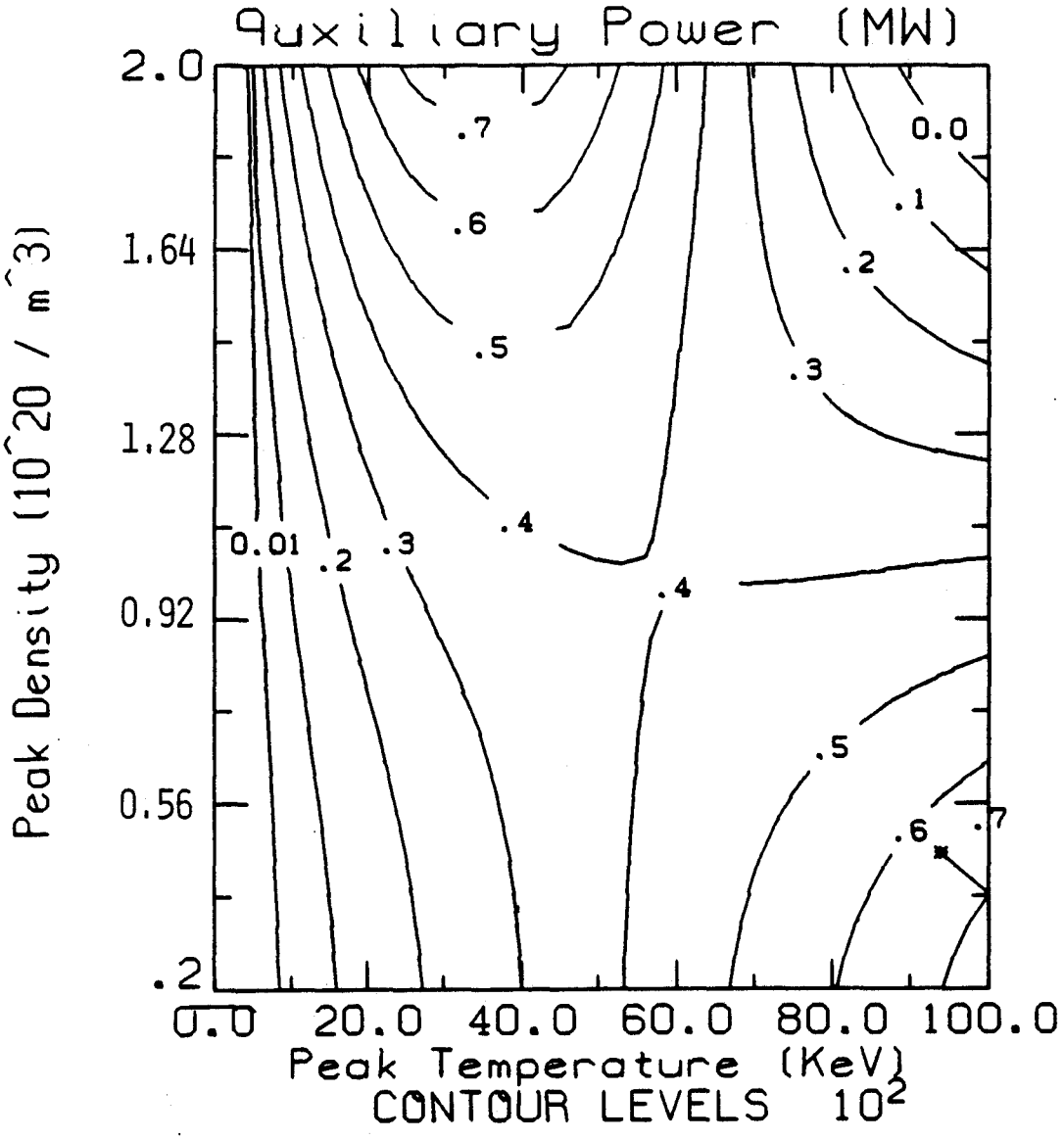

Figure 11: D-^{3}He reactor density-temperature operating space with contours of auxiliary power.

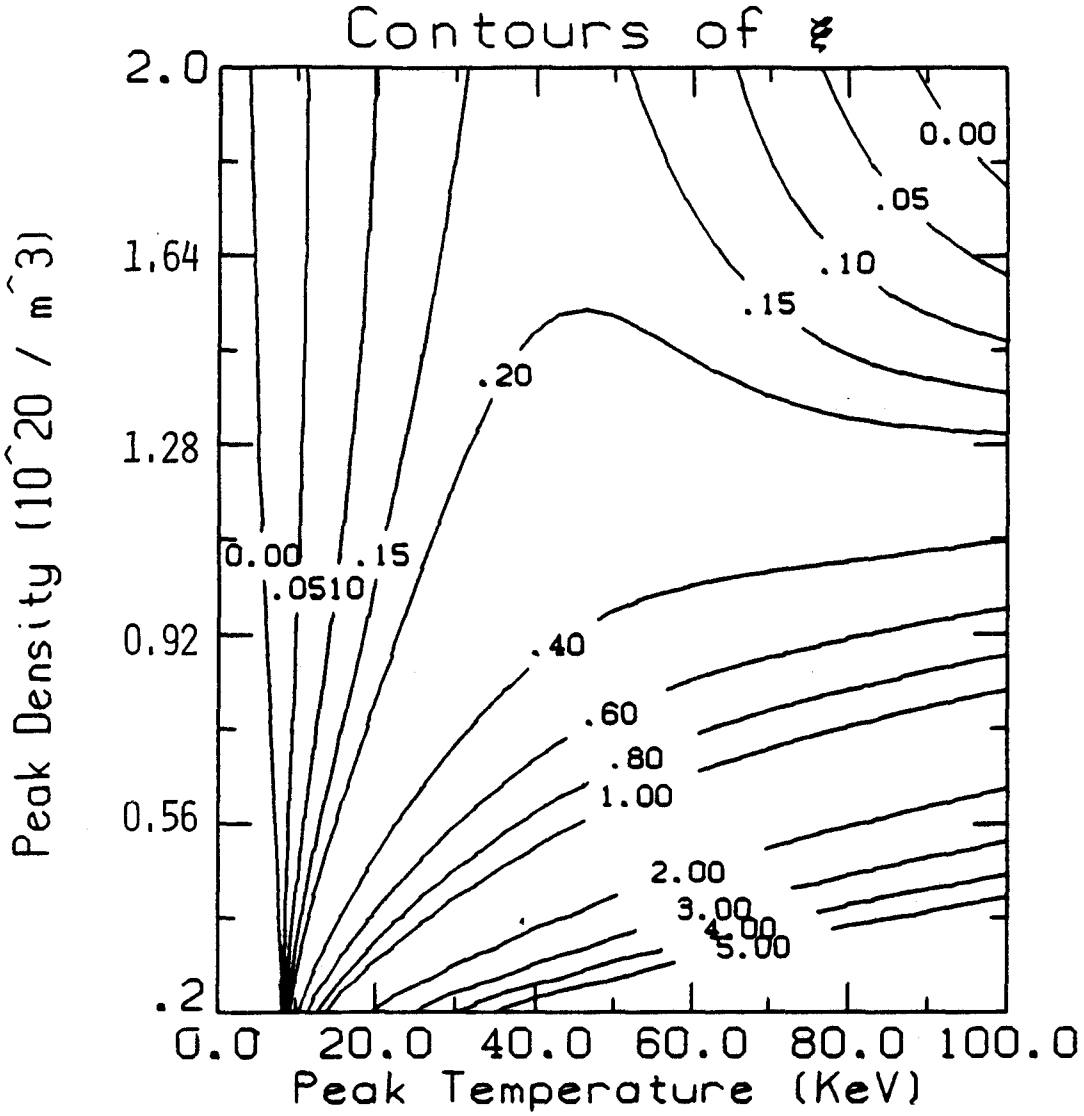

Figure 12: D-^{3}He reactor contours of constant ξ (cf. Eq. 47) for D-T fusion. The P_{ICRF} values needed in evaluating ξ are taken from Fig. 7 at each value of density and temperature.

Table 1: Parameters for the Tokamaks under consideration

Parameters		CIT	ITER	D-^{3}He
R_0	Major Radius (m)	2.6	6.0	6.3
a	Minor Radius (m)	0.8	2.15	2.0
B_0	Magnetic Field (T)	9	4.85	10
I_P	Plasma current (MA)	11.8	22	33
H	H-mode factor	1.85	1.85	4.0

in the fusion reactivity (reaction rate). In order to investigate the effect of ICRF tail heating "ξ effect" on machine performance we choose an operating point (density, temperature) and then calculate the auxiliary power required to sustain the operating point with and without the ξ effect.

In the CIT operating space (Fig. 7) we calculate the effect of ξ at the operating point $n_{e_0} = 4.2 \times 10^{20}/\mathrm{m}^3$, $T_{e_0} = 18$ keV. In order to sustain the operation at this point 24 MW of auxiliary power must be provided to the plasma if both the deuterium and tritium ion distribution functions are Maxwellian. By considering the effect of ICRF heating on the deuterium distribution function (with ξ effect) the required auxiliary power is reduced to 20.5 MW. This 14% reduction in the required auxiliary power is a consequence of the increase in the fusion power production due to the alteration of the distribution function by the ICRF heating.

In the ITER operating space (Fig. 9) the effect of ξ is calculated at the operating point $n_{e_0} = 0.6 \times 10^{20}/\mathrm{m}^3$, $T_{e_0} = 32$ keV. In this case the auxiliary power required to maintain this operating point without the ξ effect is 16.5 MW and with the ξ effect the auxiliary power is reduced by 24% to 12.5 MW.

A similar analysis is performed for the D-^{3}He tokamak. In the D-^{3}He operating space we choose the operating point $n_e = 1.0 \times 10^{20}/\mathrm{m}^3$, $T_e = 60$ keV. Sustaining operation at this point requires 36 MW of auxiliary power when no ξ effect is considered, and 28 MW with the inclusion of the ξ effect. This results in a 22% decrease in the required auxiliary power.

5 Dynamic Issues

In the previous analysis the effect of ICRF heating on the steady state plasma performance was analyzed. Due to the enhancement of the fusion reactivity the amount of auxiliary power required to sustain a given equilibrium can be reduced by 14% in CIT and by as much as 22% in a D-^{3}He reactor.

In reality, a plasma is expected to experience temperature perturbations which might need to be stabilized in order to achieve the optimum performance required by a fusion reactor. In order to model this scenario, a time dependent plasma transport model is considered. The time dependent 0-D transport model (Eq. 8) can be used to analyse the global dynamic behavior of the plasma. One way to stabilize plasma temperature fluctuations is by active auxiliary power modulation. Such a method has been considered in the past [9,10,11] finding that it can be used effectively to control both positive and negative temperature fluctuations.

As it is demonstrated in reference [10] the delay time τ_d associated with the feedback system of a burn control scheme which is based on auxiliary power modulation is closely linked to the behavior of the complete control scheme. In the present analysis the work presented in [10] is expanded to include the effects of the energy transfer between the ICRF heated tail ions and the background plasma.

In an ICRF heated plasma the tail of the resonant (heated) ions distribution function is raised thereby increasing the effective temperature of the heated species. When the ICRF power is shut-off, or when the amount of ICRF power supplied to the plasma changes, as it will happen during a burn control scenario, it takes a finite amount of time for the distribution function to achieve a new equilibrium. The new equilibrium is achieved by collisions which result in energy transfer among the plasma species. A full Fokker Plank simulation of Eq. 30 including fast alpha particle slowing down is beyond our scope. Here, a simplified analysis of a two component

plasma is considered with the background species (denoted by β) which are characterized by a Maxwellian distribution function with temperature T_β, and of test particle (denoted by α) which are characterized by "temperature" T_α. In such a plasma, the rate of change for the temperature of species α, which results from collisions between particles (α) and (β), is given in [12] as

$$\frac{dT_\alpha}{dT} = \frac{1}{\tau_\xi^{\alpha/\beta}}(T_\beta - T_\alpha) \tag{19}$$

where $\tau_\xi^{\alpha/\beta}$ is the equipartition time for the temperature

$$\tau_\xi^{\alpha/\beta} = \frac{3}{8\sqrt{2}\sqrt{\pi}} \frac{(m_\alpha T_\beta + m_\beta T_\alpha)^{3/2}}{\sqrt{m_\beta m_\alpha} Z_\alpha^2 Z_\beta^2 n_\beta \ln \Lambda_{\alpha/\beta}} \tag{20}$$

In the above equation m_j, Z_j, T_j, and n_j correspond to the mass, charge, temperature, and density of the jth particle, and $\ln \Lambda_{\alpha/\beta}$ is the Coulomb logarithm. In MKS units and for the temperature given in keV and the density in units of $10^{20}/\mathrm{m}^3$ Eq. 20 becomes

$$\tau_\xi^{\alpha/\beta} = 5.5 \times 10^{10} \frac{(m_\alpha T_\beta + m_\beta T_\alpha)^{3/2}}{\sqrt{m_\beta m_\alpha} Z_\alpha^2 Z_\beta^2 n_\beta \ln \Lambda_{\alpha/\beta}} \tag{21}$$

5.1 The complete 0-D time dependent model

The relation which describes the volume averaged (0-D) evolution of the plasma temperature is given by Eq. 8. For a given heating power, the characteristic time associated with the evolution of the global temperature is proportional to the energy confinement time τ_E. The next step in developing the complete 0-D transport model is to characterize the feedback system required for performing burn control simulations, and to determine the various delay times and characteristic times associated with the system. In

reference [10] the equations characterizing an auxiliary power burn control system are derived. These equations are: the energy balance equation, the equation characterizing the effect of fusion particle thermalization, and the equation describing the feedback system behavior. In summary these equations are:

$$\frac{dT}{dt} = \mathcal{G}(T, n, P_\alpha(n,T), P_{aux}(T_d)) \tag{22}$$

$$\frac{dP_\alpha}{dt} = \frac{1}{\tau_\alpha}[Q_\alpha(n,T) - P_\alpha(n,T)] \tag{23}$$

$$\frac{dT_d}{dt} = \frac{1}{\tau_d}[T - T_d] \tag{24}$$

where the equations describing the evolution of plasma particle density have been omitted. Equation 22 corresponds to the energy balance Eq. 8 and has been written in functional form for convenience. $\mathcal{G}$ is a function of the plasma temperature (T), the density (n), the fusion power absorbed by the plasma at time t (P_α), and the auxiliary power supplied to the plasma at time t ($P_{aux}(T_d)$). Equation 23 represents the effect of finite thermalization time for the fusion products (i.e. alpha particles in D-T fusion). Q_α represents the amount of fusion power produced at time t, P_α is the amount of fusion power absorbed by the plasma at time t, and τ_α corresponds to the fusion particle thermalization time. Equation 24 models the feedback system which is characterized by a delay time τ_d. Note that T is the temperature of the plasma at time t and T_d is the temperature that the feedback system responds to at time t. (This concept is briefly elucidated in Appendix C).

Equations 22,23,24, along with the equations characterizing the density evolution, have been used in [10] in modeling the burn control system of CIT. There it was found that the feedback delay time τ_d is strongly related to the performance of the overall control system. Depending on the value

of τ_d the feedback system can be underdamped or overdamped. An overdamped system is characterized by small τ_d ($\leq 1/10$ sec). As τ_d increases the system becomes underdamped and the smallest perturbations may result in instability particularly when τ_d becomes greater than 1-2 seconds.

For the problem at hand a simple modification must be made to the model presented by Eqs. 22-24 in order to include the effect of distribution function modification due to ICRF heating. The basic principle is that the problem is now characterized by another delay time which is a function of the change induced to the distribution function due to ICRF heating. This time delay is labeled τ_ξ and is given by Eq. 21.

When the plasma is heated by ICRF waves the energy is stored in the plasma due to the alteration of the distribution function which has an effective temperature T. If the heating is cut off the characteristic energy thermalization time of the heated ions with the background plasma is given by τ_ξ. By taking into account this phenomenon the complete burn control model is given by

$$\frac{dT}{dt} = \mathcal{G}\left(T, n, P_\alpha(n,T), P_{aux}(T)\right) \tag{25}$$

$$\frac{dP_\alpha}{dt} = \frac{1}{\tau_\alpha}\left[Q_\alpha(n,T) - P_\alpha(n,T)\right] \tag{26}$$

$$\frac{dT_d}{dt} = \frac{1}{\tau_d}\left[T - T_d\right] \tag{27}$$

$$\frac{dP_{aux}}{dt} = \frac{1}{\tau_\xi}\left(Q_{aux}(T_d) - P_{aux}(T)\right) \tag{28}$$

Here, Q_{aux} is the amount of auxiliary power deposited in the plasma at time t and P_{aux} is the amount of auxiliary power transferred to the bulk plasma at time t.

5.2 Time dependent simulations

Using Eqs. 25-28 the dynamic behavior of a D-^{3}He tokamak plasma is investigated under various temperature perturbations and for different values of the system characteristic delay times τ_d and τ_ξ.

The equilibrium about which the dynamic behavior is to be investigated is chosen from the operating space of the D-^{3}He reactor shown on Fig. 11. In particular the chosen operating point is: peak electron density $1.0 \times 10^{20}/\mathrm{m}^3$ and peak electron temperature 60 keV. At this operating point, and for the case where the distribution functions of both the deuterium and ^{3}He ions are represented by Maxwellian distribution functions, steady state operation is achieved with 36 MW of auxiliary power. By incorporating the change in the distribution function due to ICRF heating the required auxiliary power for steady state operation at the the same point is reduced to 26 MW.

Equation 28 requires the characterization of the function $Q_{aux}(T)$ which represents the feedback system response. In this analysis the relation of auxiliary power to temperature is given by

$$Q_{aux}(T) = \begin{cases} Q_{max} & T < T_1 \\ Q_{max}\left[1 - \left(\frac{T-T_1}{T_2-T_1}\right)^{\lambda}\right] & T_1 < T < T_2 \\ 0 & T > T_2 \end{cases} \tag{29}$$

The above equation represents a proportional feedback law. Q_{max} is the maximum amount of auxiliary power available. T is the temperature which the system attempts to stabilize. T_1 is a temperature below which the control system supplies the maximum amount of auxiliary power Q_{max} and T_2 is a temperature above which the the auxiliary power is zero. The exponent λ represents the rate of change of auxiliary power with temperature. In the results presented below it is assumed that $T_1 = 55$ keV, $T_2 = 67$ keV, $\lambda = 2$ and $Q_{max} = 30$ MW.

As a base case the dynamic stabilization of a D-^{3}He plasma, without the effect of ICRF heating on distribution function modification "no ξ effect", is considered first. Figure 13 shows the evolution of the global plasma temperature after a 10% temperature perturbation at time t = 0.5 sec. The feedback system responds by reducing the auxiliary power supplied to the

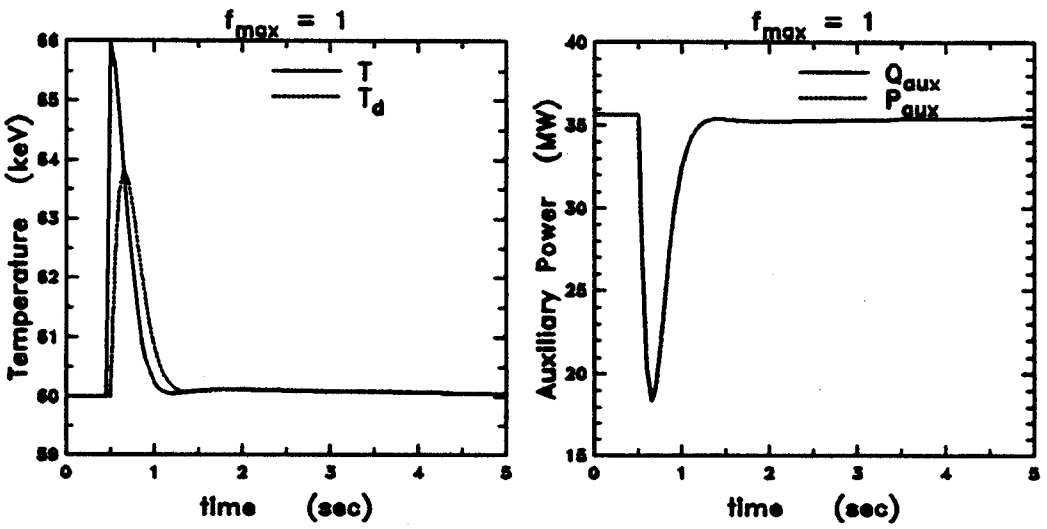

Figure 13: Stabilization of a 10% positive temperature deviation (left) with the aide of auxiliary power (right) for a D-^{3}He reactor plasma. The effect of ICRF heating on distribution function modification is not considered. The system is characterized by a feedback delay time $\tau_d = 0.1$ seconds.

plasma with a resulting decrease in temperature. The amount of auxiliary power supplied by the feedback system Q_{aux} is equal to the amount of auxiliary power transferred to the bulk plasma since the effect of heating on the distribution function is not considered. In this situation the plasma temperature equilibrates within one second of the disturbance.

In order to investigate the effect of ICRF heating on the plasma dynamics, as presented by Eqs. 25-28, the evolution of the plasma temperature following a 10% temperature perturbation is investigated under various assumptions for the characteristic time τ_ξ.

First, for $\tau_\xi = 0.1$ seconds and for $\tau_d = 0.1$ seconds the temperature and auxiliary power evolution following a perturbation is shown on Fig. 14. Note that by considering the ξ effect the system becomes underdamped as it is apparent by the overshooting and eventual stabilization of the system within two seconds of the disturbance. By increasing the characteristic time τ_ξ to 0.5 seconds (see Fig. 15). Note that in this scenario the system is further underdamped and it is eventually stabilized within 5 seconds from the disturbance.

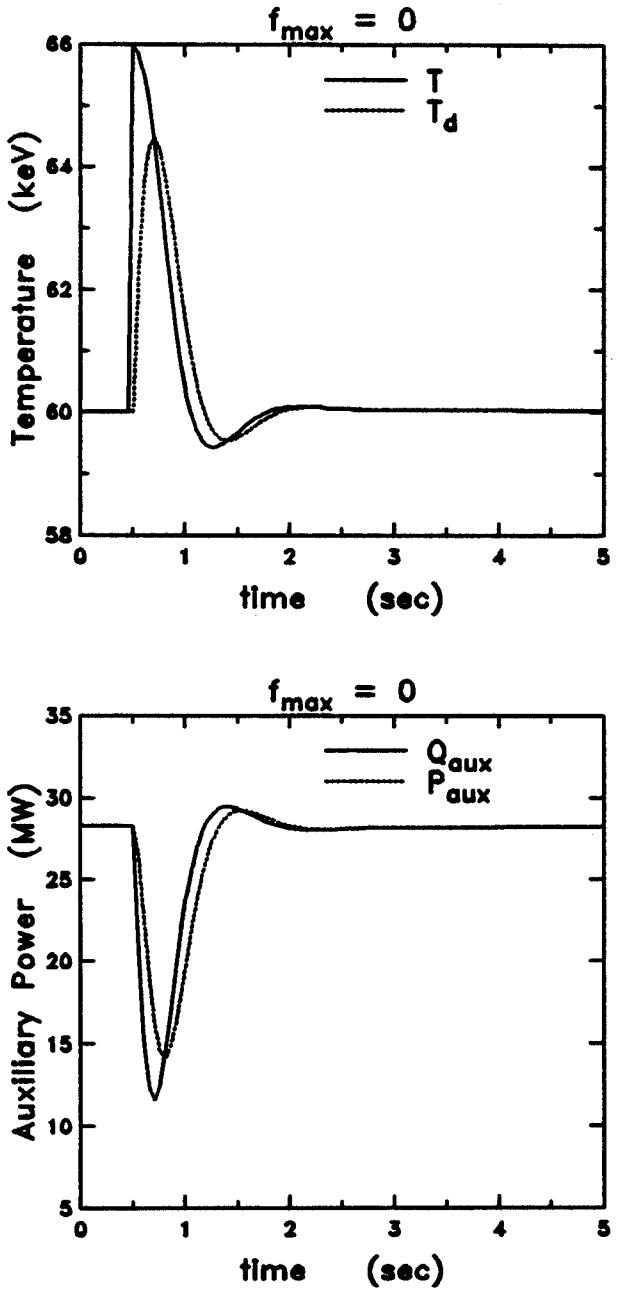

Figure 14: A plot indicating the stabilization of a 10% positive temperature deviation with the aide of auxiliary power for a D-^{3}He reactor plasma. The system is characterized by a feedback delay time $\tau_d = 0.1$ seconds and by a tail relaxation delay time τ_ξ which in this plot is set equal to 0.1 seconds. The top figure shows the temperature evolution and the bottom figure represents the evolution in the auxiliary power.

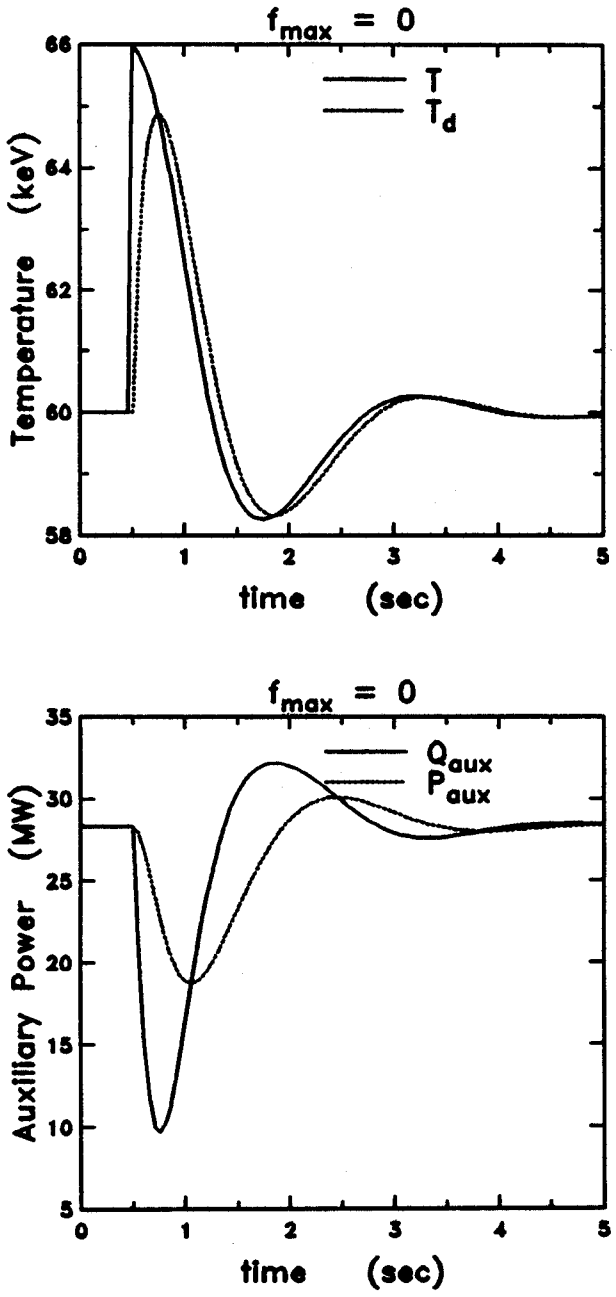

Figure 15: A plot indicating the stabilization of a 10% positive temperature deviation with the aide of auxiliary power for a D-^{3}He reactor plasma. The system is characterized by a feedback delay time $\tau_d = 0.1$ seconds and by a tail relaxation delay time τ_ξ which in this plot is set equal to 0.5 seconds. The top figure shows the temperature evolution and the bottom figure represents the evolution in the auxiliary power.

The characteristic time τ_ξ is a function of the plasma parameters as given by Eq. 21. At the equilibrium point (i.e. at $T_{e_0} = 60$ keV and $n_{e_0} = 1.0/\mathrm{m}^3$) Eq. 21 gives $\tau_\xi = 0.72$ seconds. For τ_ξ given by Eq. 21 the evolution of the plasma temperature following a 10% positive and negative temperature perturbation is shown on Fig. 16. Note that the perturbation is stabilized after substantial oscillations about the equilibrium which indicates that the system is underdamped.

In the example presented here the longest time constant in the problem is the energy confinement time τ_E. At the equilibrium of interest the energy confinement time is 11 seconds for ITER89P scaling with an H-mode factor of 4. For $\tau_\xi = \tau_E$ a simulation of the control is shown on Fig. 17. In this situation the system is severely underdamped and it takes a long time for the system to return to equilibrium.

The phenomenological variations of τ_ξ in the range $\tau_d \leq \tau_\xi \leq \tau_E$ assumed in our time response studies are intended to show the consequences of fuel ion tail heating without addressing the underlying causes for a given value of τ_ξ. In actual burning plasmas, the tail equilibration will be more complicated than given in Eqs. (21)-(19). The tail ion distribution can be modelled more accurately using a bounce averaged rf Fokker-Planck code. In addition to collisional temperature equilibration the **effective** relaxation time τ_ξ may be determined by fluctuation driven energy exchange and by less than perfect coupling of fast ions to the bulk plasma due to anomalous losses during slowing down. This coupling efficiency η_f (where f denotes fast ions including fusion products) is a quantity of great interest since it determines the power balance of the burning plasma. When $\eta_f < 1$, substantially more auxiliary power may be needed to produce the same ignition margin $n\tau T$. At present, first theoretical models of $\eta_f < 1$ are forthcoming but a predictive capability for the performance of an engineering test reactor will require crucial comparisons with experiments. One can use the time dependent modelling of the response to a temperature perturbation

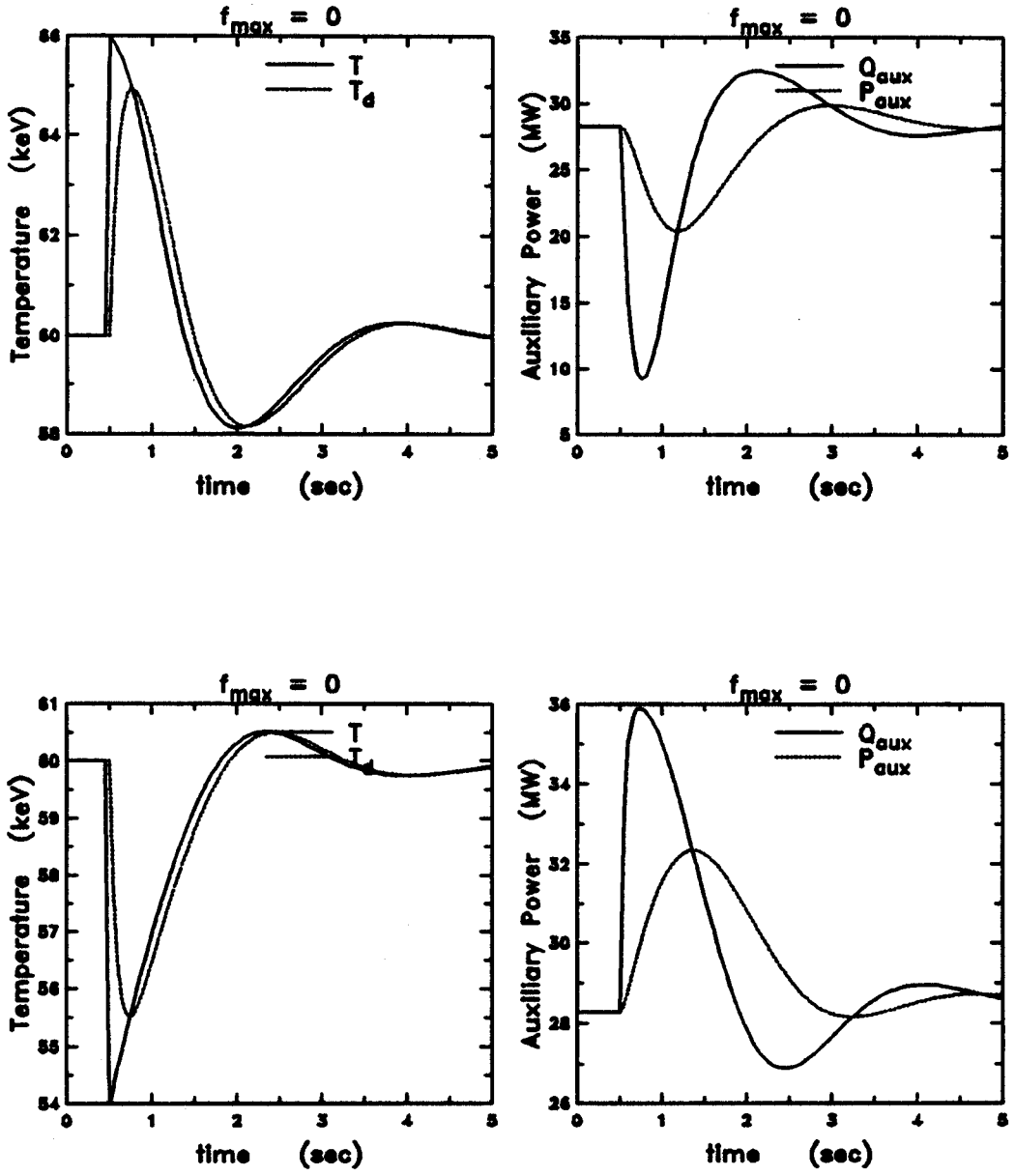

Figure 16: A plot indicating the stabilization of a 10% positive (top figure) and negative (bottom figure) temperature deviation with the aide of auxiliary power for a D-^{3}He reactor plasma. The system is characterized by a feedback delay time $\tau_d = 0.1$ seconds and by a tail relaxation delay time τ_ξ which in this plot is given by Eq. 21.

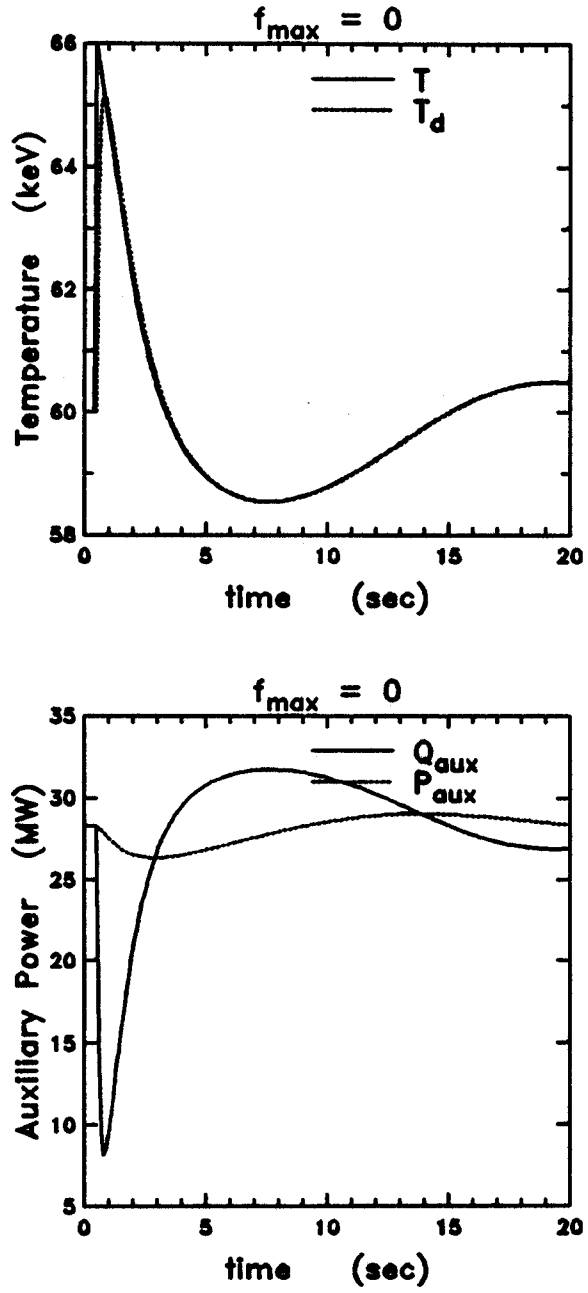

Figure 17: Stabilization of a 10% positive temperature deviation (top figure) with the aide of auxiliary power (bottom figure) for a D-^{3}He reactor plasma. The system is characterized by a feedback delay time $\tau_d = 0.1$ seconds and by a tail relaxation delay time τ_ξ which in this plot is set equal to the energy confinement time τ_E.

developed above to shed light on the magnitude of τ_α , τ_ξ (cf. Eqs. (26)-(28) and the underlying physical mechanisms, by comparing the simulation results (such as Figs. 14-17) with experimental measurements in a manner reminiscent of heat pulse propagation studies of the electron thermal conductivity χ_e using the sawtooth crash or an applied local heat pulse at the $q = 1$ surface.

6 Summary and Conclusions

When feedback control of the auxiliary heating power P_{aux} is used to provide thermal stability for an underignited fusion plasma, this heating (particularly ICR minority heating) can produce an ion tail formation which affects the fusion reactivity and hence the dynamic behavior of the plasma operating point.

Using the Stix formula for the ion tail formation due to ICR minority heating we find substantial tail formation, i.e., the Stix parameter ξ (cf. Eq. (2)) is ≤ 1 for typical operating points in CIT and ITER, and $\xi \geq 1$ in a D- ^{3}He reactor. For $T = 10$ keV in CIT and ITER this produces a fusion reactivity enhancement by a factor of ~ 1.5, and at $T = 50$ keV in the D- ^{3}He reactor by a factor of ~ 3.0. In steady state at finite Q below ignition, this enhancement corresponds to a reduction of required P_{aux} of $\approx 14\%$ in CIT, 24% in ITER and 22% in the D- ^{3}He reactor.

Extending this approach to the time dependent volume averaged (0-D) power balance we have presented a dynamic feedback model based on controlling P_{aux} with a time delay τ_d (reflecting not only the feedback circuit response but also the finite response time needed for a sudden adjustment of the heating power source). In addition to τ_d the model (Eqs. 25-28) depends on the effective fusion power thermalization time τ_α (which may be affected by anomalous fast α diffusion losses) and the effective tail ion thermalization time τ_ξ (similarly affected by classical and possible anomalous processes).

Increasing τ_ξ/τ_d increases the phase lag between the power Q_{aux} applied to the plasma and the power P_{aux} absorbed by the plasma, at a given time t, leading to an increasingly underdamped behavior of P_{aux} as well as the plasma temperature T. For $\tau_\xi = \tau_E$, the damping time of these oscillations is several times τ_E in the D-^{3}He reactor used here to demonstrate the effect.

Temperature excursions and the ensuing oscillations induce fluctuations in fusion power which may effect the fatigue characteristics of the mechanical components surrounding the plasma. In order to evaluate the magnitude of this effect a comparison between the frequency of the oscillations and the time constant which introduces adverse thermal cycling effects must be made.

Besides the consequences of these oscillations on the operating characteristics, the shape of the temperature excursions can be used to reveal and analyze the physical features of the underlying anomalous transport mechanisms determining τ_α and τ_ξ which need to be understood to predict the burning plasma performance.

Acknowledgments

The authors would like to thank Professor Jeff Freidberg for useful discussions during the preparation of this paper. This work was sponsored by U. S. DoE grant DE-FG02-91ER-54109.

Appendix A: Theory of Tail Formation due to ICRF Heating

The bounce averaged Fokker-Plank equation is given by

$$\frac{\partial \langle f \rangle}{\partial t} = \frac{1}{\tau_B} \int [\mathcal{C}(f) + \mathcal{Q}(f)] \frac{d\ell}{|v_\parallel|} \tag{30}$$

where $\mathcal{C}$ corresponds to the local collision operator and $\mathcal{Q}$ represents the local quasi-linear diffusion operator due to ICRF heating. τ_B is the particle bounce period and is given by

$$\tau_B = \int \frac{d\ell}{|v_\parallel|} \tag{31}$$

and $\langle \quad \rangle$ represents the bounce averaging operator. Eq. 30 becomes

$$\langle \frac{\partial f}{\partial t} \rangle = \langle \mathcal{C}(f) \rangle + \langle \mathcal{Q}(f) \rangle \tag{32}$$

The bounce averaged collision operator, $\mathcal{C}$, may be written as

$$\langle \mathcal{C}(f) \rangle = \langle \frac{\partial}{\partial v} \Gamma(f) \rangle \tag{33}$$

where Γ signifies a flow in velocity space which, if pitch angle scattering and slowing down of fusion products is neglected, is simply

$$\Gamma = \sum_j \lambda_j A_j(v) \frac{1}{v^2} \left[\frac{v_j^2}{2v} \frac{\partial f}{\partial v} + \frac{m}{m_j} f \right] \tag{34}$$

with the subscript j representing the background plasma species. m is the mass of the minority ion. The parameters λ_j and A_j are given by

$$\lambda_j = \frac{4\pi e^4 Z^2 Z_j^2 n_j \ln \Lambda}{m^2} \tag{35}$$

$$A_j = \frac{2}{\sqrt{\pi}} \int_0^{v/v_j} \sqrt{x} \exp(-x)\, dx \tag{36}$$

$$\simeq \frac{2/(3\sqrt{\pi})\,(v/v_j)}{1 + 4/(3\sqrt{\pi})\,(v/v_j)^3} \tag{37}$$

The quasi-linear operator $\mathcal{Q}$ is given by

$$\mathcal{Q}(f) = \frac{\partial}{\partial v} \mathcal{D} \frac{\partial f}{\partial v} \tag{38}$$

The diffusion coefficient $\mathcal{D}$ is given in reference [13], and upon bounce averaging it becomes

$$\mathcal{D} = \frac{1}{\tau_B} \frac{2}{3m} \langle \delta E_\perp \rangle \tag{39}$$

where $\delta E_\perp$ is the change in particle energy due to its interaction with the wave. In terms of the ICRF absorbed power density $\langle P \rangle$ the diffusion coefficient $\mathcal{D}$ can be expressed as

$$\mathcal{D} = \frac{\langle P \rangle}{3\, n\, m} \tag{40}$$

where n and m are the density and mass of the resonating (heated) particles.

Finally by substituting Eqs. 33 and 38 into Eq. 32 and dropping the bounce average operator $\langle\ \ \rangle$, the isotropic part of the Fokker-Plank equation becomes

$$\frac{\partial f}{\partial t} = \frac{\partial}{\partial v} \left[\sum_j \lambda_j A_j(v) \frac{1}{v^2} \left(\frac{v_j^2}{2v} \frac{\partial f}{\partial v} + \frac{m}{m_j} f \right) + \mathcal{D} \frac{\partial f}{\partial v} \right] \tag{41}$$

In steady state ($\partial f / \partial t = 0$) Eq. 41 is integrated twice with the result

$$\ln f(v) = -\int_0^v \frac{\sum_j \lambda_j A_j m/m_j}{\sum_j \lambda_j A_j v_j/(2v) + \mathcal{D} v^2} dv \tag{42}$$

With further algebraic manipulation of the above integral, the velocity distribution function of the resonant ions can be written as

$$f(v) = n\left(\frac{m}{2\pi T_e}\right)^{3/2} \exp\left[-\frac{mv^2}{2T_e}\mathcal{F}(\xi)\right] \tag{43}$$

Note that the above expression for the distribution function represents a Maxwellian distribution modified by the function $\mathcal{F}$. The function $\mathcal{F}$ is given by [2]

$$\mathcal{F} = \frac{1}{1+\xi}\left[1 + \frac{R_j(T_e - T_j + \xi T_e)}{T_j(1+R_j+\xi)} H(E/E_j)\right] \tag{44}$$

In the above equation T_e corresponds to the electron temperature and T_j represents the temperature of the background ions. ξ is a dimensionless parameter which represents the effect of wave heating on the shape of the distribution function of the resonant ions and is given by

$$\xi = \mathcal{D}\frac{m^2 v_e}{2/(3\sqrt{\pi})4\pi n_3 e^4 Z^2 \ln\Lambda} \tag{45}$$

which according to Eq. 40 becomes

$$\xi = \frac{m\langle P\rangle}{8\sqrt{\pi} n_e n Z^2 e^4 \ln\Lambda}\left(\frac{2T_e}{m_e}\right)^{1/2} \tag{46}$$

Here, $\langle P\rangle$ represents the ICRF heating power per unit volume delivered to the resonant ions, Z is the charge of the resonant ions, and $\ln\Lambda$ is the plasma Coulomb logarithm. In MKS units and with the temperature T_e given in keV and the densities n_e, n in units of $10^{20}/\mathrm{m}^3$ Eq. 46 becomes

$$\xi = 1.68\times 10^6 \frac{m\langle P\rangle}{n_e n Z^2 \ln\Lambda}\left(\frac{2T_e}{m_e}\right)^{1/2} \tag{47}$$

The parameters R_j, E_j and H in Eq. 44 are given by

$$R_j = \frac{n_j Z_j^2}{n_e} \left(\frac{m_j}{m_e} \frac{T_e}{T_j} \right)^{1/2} \tag{48}$$

$$E_j = \frac{m}{m_j} T_j \left[\frac{3\sqrt{\pi}(1 + R_j + \xi)}{4(1 + \xi)} \right]^{2/3} \tag{49}$$

$$H(x) = \frac{1}{x} \int_0^x \frac{du}{1 + u^{3/2}} \tag{50}$$

Appendix B: Cross Sections for D-T and D-^{3}He Reactions

The Deuterium Tritium reaction cross section is given by [14]

$$\sigma(E) = \frac{a_0 + E(a_1 + E(a_2 + Ea_3))}{1 + E(b_1 + E(b_2 + Eb_3))} \frac{1}{E \exp[B/\sqrt{E} - 1]} \tag{51}$$

The parameters a_j and b_j assume the values

$$a_0 = 1.15 \times 10^{-24} \tag{52}$$

$$a_1 = 1.39 \times 10^{-26} \tag{53}$$

$$a_2 = 1.50 \times 10^{-28} \tag{54}$$

$$a_3 = -1.607 \times 10^{-31} \tag{55}$$

$$b_1 = -1.908 \times 10^{-4} \tag{56}$$

$$b_2 = -4.306 \times 10^{-4} \tag{57}$$

$$b_3 = 7.276 \times 10^{-6} \tag{58}$$

$$B = 34.3828 \tag{59}$$

With the above parameters and with the energy E given in keV the cross section σ is given in m^2 and it is accurate to 3% up to energies of 250 keV.

The Deuterium Helium 3 reaction cross section is given by [15]

$$\sigma(E) = \frac{a_1}{1 + E(b_1 + E(b_2 + Eb_3))} \frac{1}{E \exp[B/\sqrt{E} - 1]} \tag{60}$$

where

$$a_1 = 5.91 \times 10^{-25} \tag{61}$$

$$b_1 = -7.85 \times 10^{-3} \tag{62}$$

$$b_2 = 2.64 \times 10^{-5} \tag{63}$$

$$b_3 = -1.42 \times 10^{-8} \tag{64}$$

$$B = 68.765 \tag{65}$$

Appendix C: A Simple Feedback Model

The question is how to choose a temporal evolution for the applied auxiliary heating power $P_{aux} = P_{aux}(t)$ such that a spontaneous temperature excursion ΔT introduced at $t = O^+$ leads to a damped oscillation of the plasma temperature. A simple choice is

$$\frac{dT}{dt} = S + P_{aux}[T_d(t)] \tag{66}$$

where S denotes all other power sources and sinks. In equilibrium,

$$O = S + P_{aux}(T_d = 0). \tag{67}$$

The "delayed temperature" T_d is chosen to obey

$$\frac{dT_d}{dt} = \frac{1}{\tau_d}(T - T_d) \tag{68}$$

where the constant delay time τ_d is determined by the feedback mechanisms and the characteristic confinement and energy equilibration times of the plasma (which may, in reality, depend on T, themselves.)

We perform a perturbation analysis $T = T_0 + \tilde{T}$, $T_d = T_0 + \tilde{T}_d$. The initial conditions are, at $t = 0$

$$T = T_d = T_0 \tag{69}$$

$$\tilde{T}_d(0) = 0, \quad \tilde{T}(0) = \Delta T \tag{70}$$

where ΔT is a sudden jump in temperature. Thus, for a small perturbation ΔT

$$P_{aux}(T_d) = P_{aux}(T_0) + \frac{\delta P_{aux}}{\delta T_d}|_{T_0}(T_d - T_0) \tag{71}$$

so that

$$\frac{d\tilde{T}}{dt} = \frac{\partial P_{aux}}{\partial T_d}|_{T_0}\tilde{T}_d \tag{72}$$

and

$$\frac{d\tilde{T}}{dt} = \frac{1}{\tau_d}(\tilde{T} - \tilde{T}_d). \tag{73}$$

The feedback law 72 is chosen such that $\left(\frac{\partial P_{aux}}{\partial T_d}\right)_{T_0} < 0$. The delayed response law 73 is chosen to be linear. From Eqs. 72, 73

$$\frac{d^2\tilde{T}_e}{dt^2} + \frac{1}{\tau_d}\frac{d\tilde{T}_e}{dt} - \frac{1}{\tau_d}\left(\frac{\partial P_{aux}}{\partial T_d}\right)_{T_0}\tilde{T}_d = 0 \tag{74}$$

which is a damped harmonic oscillator, as desired, with oscillation frequency $\left[-\frac{1}{\tau_d}\left(\frac{\partial P_{aux}}{\partial T_d}\right)_{T_0}\right]^{1/2}$. From 74 one can see that while $T(t)$ jumps by ΔT and then decays, $T_d(t)$ first rises and, after a delay, decays also.

References

[1] J.M. Dawson, H.P. Furth, and F.H. Tunney. Production of Thermonuclear Power by Non-Maxwellian Ions in a Closed Magnetic Field Configuration. *Physical Review Letters*, 26:1156–1160, 1971.

[2] T.H. Stix. Fast Wave Heating of a Two-Component Plasma. *Nuclear Fusion*, 15:737–754, 1975.

[3] J. Kesner. Quasi-Linear Model for Ion Cyclotron Heating of Tokamaks and Mirrors. *Nuclear Fusion*, 18:781, 1978.

[4] D. T. Blackfield and J.E. Scharer. Anisotropy and Tail Formation in ICRF-Heated Plasmas. *Nuclear Fusion*, 22:255, 1982.

[5] J.E. Scharer, J. Jackquinot, P. Lallia, and F. Sand. Fokker-Plank Calculations for JET ICRF Heating Scenarios. *Nuclear Fusion*, 25:435, 1985.

[6] R. W. Harvey, M. G. McCoy, G. D. Kerbel, and S. C. Chiu. ICRF Fusion Reactivity Enhancement in Tokamaks. *Nuclear Fusion*, 26:43, 1986.

[7] R.R. Parker et al. Progress in Tokamak Research at MIT. *Nuclear Fusion*, 25(3), 1985.

[8] ITER Physics Design Guidlines. Technical report, IAEA, Vienna, 1990.

[9] E. A. Chaniotakis et al. CIT Burn Control Using Auxiliary Power Modulation. Technical Report PFC/RR-89-16, Massachusetts Institute of Technology, 1989.

[10] E.A. Chaniotakis. *Ignition and Burn Control Characteristics of Thermonuclear Plasmas.* PhD thesis, Massachusetts Institute of Technology, 1990.

[11] L. Bromberg J. L. Fisher D. R. Cohn. Active burn control of ignited plasmas. *Nuclear Fusion*, 20(2), 1980.

[12] B. A. Trubnikov. *Particle Interactions in a Fully Ionized Plasma*, volume 1 of *Reviews of Plasma Physics*, pages 105–204. Consultants Bureau, New York, 1965.

[13] C.F. Kennel and F. Engelmann. Velocity Space Difusion fron Weak Plasma Turbulence in a Magnetic Field. *Physics of Fluids*, 9:2377–2388, 1966.

[14] G. Sadler and P van Belle. Fusion Cross Sections and Reactivities. Technical report, JET, 1989.

[15] Asher Peres. Fusion Cross Sections and Thermonuclear Reaction Rates. *Journal of Applied Physics*, 50:5569–5571, 1979.